

1 Transplantation of high fat fed mouse microbiota into zebrafish embryos identifies pathobiont  
2 species

3

4 Pradeep Manuneedhi Cholan<sup>1</sup>, Simone Morris<sup>1</sup>, Kaiming Luo<sup>1</sup>, Jinbiao Chen<sup>2</sup>, Jade A Boland<sup>2</sup>, Geoff  
5 W McCaughan<sup>2,3</sup>, Warwick J Britton<sup>1,4</sup>, Stefan H Oehlers<sup>1,5</sup> \*

6 <sup>1</sup> Tuberculosis Research Program at the Centenary Institute, The University of Sydney,  
7 Camperdown, NSW 2050, Australia

8 <sup>2</sup> Liver Injury and Cancer Program at the Centenary Institute, The University of Sydney,  
9 Camperdown, NSW 2050, Australia

10 <sup>3</sup> AW Morrow Gastroenterology and Liver Centre, Royal Prince Alfred Hospital, Camperdown, NSW  
11 2050, Australia

12 <sup>4</sup> Department of Clinical Immunology, Royal Prince Alfred Hospital, Camperdown, NSW 2050,  
13 Australia

14 <sup>5</sup> The University of Sydney, Discipline of Infectious Diseases & Immunology and Marie Bashir  
15 Institute, Camperdown, NSW 2050, Australia

16

17

18 Corresponding author: Dr Stefan Oehlers [stefan.oehlers@sydney.edu.au](mailto:stefan.oehlers@sydney.edu.au)

19 ORCID: 0000-0003-0260-672X Twitter: @oehlerslab

20

21 Keywords: zebrafish, hyperlipidaemia, microbiota, pathobiont, myd88

22

## 23 **Abstract**

24 Gut dysbiosis is an important modifier of pathologies including cardiovascular disease but our  
25 understanding of the role of individual microbes is limited. Here, we have used transplantation of

26 mouse microbiota into microbiota-deficient zebrafish embryos to study the interaction between  
27 members of a mammalian high fat diet-associated gut microbiota with a lipid rich diet challenge in  
28 a tractable model species. We find zebrafish embryos are more susceptible to hyperlipidaemia  
29 when colonised with mouse high fat-diet-associated microbiota and that this effect can be driven  
30 by individual bacterial species. Colonisation or exposure to *Enterococcus faecalis* activates host  
31 Myd88 signalling, an effect that is phenocopied by the Gram positive Toll-like receptor agonists  
32 peptidoglycan and lipoteichoic acid, to drive hyperlipidaemia. In contrast, we find  
33 *Stenotrophomonas maltophilia* increases the hyperlipidaemic potential of chicken egg yolk  
34 independent of gut colonisation. In this work, we demonstrate the applicability of zebrafish as a  
35 tractable host for the identification of gut pathobionts via microbiota transplantation and  
36 subsequent challenge with a high fat diet.

37

## 38 **Introduction**

39 The metagenome encoded by the gut microbiome is an essential component of the animal  
40 digestive system <sup>1,2</sup>. Microbes can affect digestion directly through the breakdown of indigestible  
41 material such as fibre to short chain fatty acids and indirectly by stimulating the differentiation of  
42 the intestinal epithelium.

43

44 The microbiome is shaped by host and environment selective pressures <sup>3,4</sup>. Lipid-rich Western  
45 diets that cause obesity in susceptible individuals are associated with gut dysbiosis which can drive  
46 an unwanted increase in nutrient absorption and epithelial leakiness <sup>5</sup>. Transplantation of human  
47 lean and obese microbiota into germ-free mice transmits these phenotypes across host  
48 mammalian species <sup>6</sup>. While the germ-free mouse has been invaluable for the study of host-  
49 microbe interactions through gnotobiotic and transplantation studies, there is a need for faster

50 and more accessible models that can act as function screening tools for disease-associate  
51 microbiota.

52

53 Zebrafish embryos require microbial colonisation during development for full physiological  
54 digestive function and are a simple platform for studying host-microbiota-environment  
55 interactions <sup>7,8</sup>. Zebrafish embryos develop *ex vivo* within a chorion that can be surface sterilised  
56 and are tolerant of antibiotics in their media making them a technically simple model for raising  
57 germ-free experimental subjects. Probiotic transfer has been shown to increase resistance to  
58 pathogen colonisation <sup>9</sup>. The zebrafish gut microbiome is sensitive to HFD challenge <sup>3</sup>.

59

60 Microbiota transplantations have been previously performed from mice and humans to zebrafish  
61 demonstrating the feasibility of using the zebrafish as an *in vivo* screening tool for studying the  
62 effects of defined microbiota on host physiology <sup>10</sup>. Here we use this technically simple model to  
63 rapidly identify specific members of the mouse HFD-associated microbiota that accelerate a diet-  
64 induced hyperlipidaemic phenotype in zebrafish embryos and the mechanisms by which these  
65 pathobionts interact with the zebrafish host.

66

## 67 **Results**

### 68 Transplantation of microbiota from HFD fed mice accelerates hyperlipidaemia in zebrafish 69 embryos

70 Microbiome-depleted (MD) zebrafish embryos were exposed to mouse faecal microbiota  
71 preparations generated from mice fed a conventional chow diet or HFD from 3-5 dpf (days post  
72 fertilization) and challenged with chicken egg yolk feeding from 5-7 dpf (Figure 1A).

73

74 We first investigated if colonisation with the control or HFD-associated mouse microbiota affected  
75 zebrafish embryo intestinal physiology at 5 dpf before the onset of exogenous feeding. The  
76 absorptive activity of zebrafish midgut lysosome-rich intestinal epithelial cells requires microbial  
77 colonisation and is impeded by inflammation<sup>11,12</sup>. We used neutral red staining visually to  
78 examine the absorptive function of colonised embryos and observed higher staining in 5 dpf  
79 embryos colonised with the HFD fed microbiota compared to chow diet colonised controls (Figure  
80 1B and 1C).

81

82 We next collected colonised zebrafish embryos one and two days after exposure to the chicken  
83 egg yolk challenge and stained with Oil Red O to visualise neutral lipids (Figure 1D). Zebrafish  
84 embryos colonised with the faecal microbiota from HFD fed mice had more vascular Oil Red O  
85 staining after 2 day of compared to zebrafish embryos colonised with the faecal microbiota from  
86 chow diet fed mice (Figure 1E)

87

88 These data demonstrate the responsiveness of MD zebrafish embryos to the transferable effects  
89 of dysbiotic mammalian gut microbiome-associated microbiota when challenged with a complex  
90 environmental stimulus in the form of lipid-rich feeding.

91

#### 92 Identification of individual microbes with pathobiont activity

93 To isolate individual species that would be amenable to *in vitro* handling and growth, faecal  
94 homogenate supernatants were plated on LB agar and grown at 28°C to select for species that  
95 would be easily handled and most likely to colonise zebrafish embryos (Figure 2A). The best  
96 growing isolate in LB broth culture from two chow diet and HFD fed faecal preparations were  
97 selected and sequenced. We identified *Enterococcus faecalis* strain YN771 (*E.f*) and  
98 *Stenotrophomonas maltophilia* strain CD103 (*S.m*) from HFD-fed mouse faecal lysate, and

99 *Escherichia* species PYCC8248 (*E.s*) and *Escherichia coli* strain Y15-3 (*E.c*) from chow diet-fed  
100 mouse faecal lysate.

101

102 We colonised MD zebrafish embryos with individual isolates to determine if specific pathobionts  
103 from HFD-fed mouse microbiomes could phenocopy the effects of bulk microbiota transfer.  
104 Gnotobiotic zebrafish embryos colonised with *E. faecalis* or *S. maltophilia* had increased Oil Red O  
105 staining compared to embryos colonised with either of the *Escherichia* strains (Figure 2B).

106

107 Interestingly, colonisation with *E. faecalis* or *S. maltophilia* did not increase the absorptive activity  
108 of the midgut intestinal epithelium compared to embryos colonised with either of the *Escherichia*  
109 strains suggesting the absorptive phenotype seen in bulk microbiota transplant is the product of  
110 multiple microorganisms (Figure 2C).

111

112 We next sought to confirm our observations using a second strain of each bacterial species, *E.*  
113 *faecalis* UNSW 054400 type strain (*E.f* UNSW) and *S. maltophilia* yy01 (*S.m* yy01) isolated from  
114 another mouse in the same facility. Colonisation of MD zebrafish embryos with either strain  
115 phenocopied the hyperlipidaemic phenotype seen with our original isolates (Figure 2D). Some  
116 variability was observed between strains of the same species suggesting strain-specific effects in  
117 our zebrafish embryo system.

118

119 Together this data demonstrates gnotobiotic zebrafish embryos can be used to identify individual  
120 pathobionts from the microbiomes of diet-challenged mice.

121

122 *Enterococcus faecalis* accelerates hyperlipidaemia by activating host immune signalling pathways

123 To investigate the mechanisms by which *E. faecalis* and *S. maltophilia* accelerate diet-induced  
124 hyperlipidaemia in zebrafish embryos, we first asked if these bacteria needed to be alive to exert  
125 their pathobionic effect. We adapted our gnotobiotic methodology to expose MD embryos to heat  
126 killed bacterial preparations prior to chicken egg yolk feeding (Figure 3A).

127

128 Exposure to heat-killed *E. faecalis* phenocopied the live *E. faecalis* hyperlipidaemic phenotype  
129 when compared MD embryos that had been exposed to either heat killed *S. maltophilia* or either  
130 of the *Escherichia* strains (Figure 3B). Conversely, heat-killed *S. maltophilia* did not induce  
131 hyperlipidaemia in concert with chicken egg yolk challenge.

132

133 Host innate immune signalling via the Myd88 adaptor protein is essential for the zebrafish  
134 intestinal epithelium to respond to microbial colonisation<sup>13</sup>. We performed knockdown of host  
135 *myd88* expression using multiple CRISPR-Cas9 gRNAs (Figure 3C). Host *myd88* expression was  
136 necessary for transducing the *E. faecalis*-induced hyperlipidaemic signal as *myd88* crispants had  
137 significantly less Oil Red O staining than scrambled gRNA/Cas9-injected control embryos after  
138 colonisation with *E. faecalis* and chicken egg yolk challenge (Figure 3D).

139

#### 140 Gram positive cell wall components accelerate hyperlipidaemia in zebrafish embryos

141 *E. faecalis* is a Gram-positive bacterium. To determine if *E. faecalis*-driven hyperlipidaemia was  
142 due to a conserved Gram-positive cell wall component, we initially compared the hyperlipidaemic  
143 potential of heat-killed *E. faecalis* to heat killed *Staphylococcus xylosus* (*S.x*), another Gram-  
144 positive bacterium obtained from the faecal microbiota of a mouse from the same facility. We  
145 found exposure to heat-killed *S. xylosus* phenocopied the hyperlipidaemic effect of heat-killed *E.*  
146 *faecalis* after chicken egg yolk challenge (Figure 4A).

147

148 Next we directly soaked MD embryos in a sublethal dose of 25 µg/mL purified lipoteichoic acid  
149 (LTA) or peptidoglycan (PGL), which are major components of the Gram-positive cell wall, prior to  
150 challenge with chicken egg yolk feeding <sup>14</sup>. Either one of these purified ligands were able to  
151 accelerate hyperlipidaemia in MD embryos (Figure 4B).

152

153 To test the requirement for intact *E. faecalis* PGL to accelerate hyperlipidaemia, we exposed MD  
154 embryos to lysozyme-digested heat-killed *E. faecalis* prior to chicken egg yolk feeding. Lysozyme  
155 digestion ablated the ability of heat-killed *E. faecalis* to accelerate hyperlipidaemia (Figure 4C).

156

157 To determine if host innate immune signalling via the Myd88 adaptor protein transduced the LTA  
158 or PGL-induced signal that accelerates hyperlipidaemia, we again knocked down *myd88* using a  
159 pooled CRISPR-Cas9 gRNA approach and exposed crispant embryos to LTA or PGL. Depletion of  
160 host *myd88* ablated the sensitivity of embryos to LTA and PGL-induced accelerated  
161 hyperlipidaemia (Figure 4D).

162

163 Together, these experiments demonstrate zebrafish embryo lipid metabolism is sensitive to the  
164 presence of Gram-positive bacterial cell wall components via Myd88-mediated host signalling  
165 pathways.

166

#### 167 *Stenotrophomonas maltophilia* accelerates hyperlipidaemia by digesting food

168 Since we had previously shown *S. maltophilia* needed to be alive to accelerate hyperlipidaemia,  
169 we hypothesised *S. maltophilia* might interact with the chicken egg yolk independently of the host  
170 colonisation. To test this hypothesis, we incubated chicken egg yolk with each of our 4 bacterial  
171 isolates in conditions representative of the zebrafish embryo media and then sterilised the “pre-  
172 digested” chicken egg yolk by autoclaving prior to feeding to MD zebrafish embryos (Figure 5A).

173

174 Compared to either untreated chicken egg yolk, autoclaved chicken egg yolk, or chicken egg yolk  
175 incubated with the other three bacterial isolates, the chicken egg yolk that had been incubated  
176 with *S. maltophilia* increased hyperlipidaemia in zebrafish embryos (Figure 5B).

177

178 We next repeated this experiment in conventionally raised embryos and found the increased  
179 hyperlipidaemic potential of *S. maltophilia* “pre-digested” chicken egg yolk was independent of  
180 colonisation by commensal microbes (Figure 5C). To examine the substrate specificity of *S.*  
181 *maltophilia*, we incubated commercially available fish embryo food with *S. maltophilia* and  
182 observed an increase in body size of embryos fed the “pre-digested” commercial feed compared  
183 to untreated commercial feed (Figure 5D).

184

185 Visual inspection of *S. maltophilia* “pre-digested” chicken egg yolk suspensions suggested *S.*  
186 *maltophilia* had broken apart the chicken egg yolk resulting in smaller particles that could be more  
187 easily ingested and altered the biochemical properties of the chicken egg yolk as the solution  
188 contained much finer particles than for other treatments (Figure 5E). An intermediate phenotype  
189 was seen in chicken egg yolk that had been “pre-digested” by *E. coli* strain Y15-3. CFU recovery  
190 assays demonstrated higher growth of *S. maltophilia* than *E. coli* strain Y15-3 suggesting the better  
191 growth of *S. maltophilia* may convert chicken egg yolk into components that could be digested by  
192 zebrafish embryos (Figure 5F). We performed nutritional panel and free fatty acid analyses of  
193 chicken egg yolk that had been “pre-digested” by *S. maltophilia* or *E. coli* strain Y15-3 as an  
194 additional control. Fatty acid analysis revealed an increase in total fat content, made up of  
195 monounsaturated and saturated fatty acids, in *S. maltophilia*-incubated samples that was not seen  
196 in control or *E. coli* strain Y15-3-incubated samples (Table 1).

197



198 These data illustrate an intestinal colonisation-independent mechanism by which *S. maltophilia*  
199 may enhance lipid uptake in zebrafish embryos by increasing the lipid content and decreasing the  
200 physical size of food.

201

## 202 **Discussion**

203 Our study demonstrates the utility of the gnotobiotic zebrafish platform to screen donor  
204 microbiota samples for transplantable biological activities in combination with an exogenous  
205 environmental factor. The addition of an exogenous trigger to the experimental system is an  
206 important permutation that allows the identification of pathobionts whose disease-associated  
207 interactions with the host only become apparent in combination with an environmental challenge  
208 such as diet.

209

210 We applied the gnotobiotic zebrafish platform to the diet-hyperlipidaemia axis as there is a  
211 growing interest in microbiome studies within the cardiovascular disease field<sup>15</sup>. The gnotobiotic  
212 zebrafish platform represents a disruptive technology that could be used to identify additional  
213 pathobiont species from human cardiovascular disease patients and as a “first pass” platform in  
214 mechanistic studies to link these species to cardiovascular pathology in mammalian systems.

215

216 Our investigation of *E. faecalis*-accelerated hyperlipidaemia uncovered a surprising role of Gram-  
217 positive cell wall component-triggered Myd88 signalling in zebrafish embryo lipid metabolism. The  
218 presence of this response in zebrafish embryos has broad implications for the use of zebrafish  
219 embryos to study transplanted mammalian microbiota as it may not be representative of the  
220 mammalian response to colonisation with Gram positive organisms. Most zebrafish embryo mono-  
221 association studies have been carried out with Gram negative organisms including *E. coli*, *A.*  
222 *veronii*, *V. cholerae*, and *P. aeruginosa*<sup>16-18</sup>.

223

224 The comparison of heat killed *E. faecalis* to heat killed *S. xylosus* demonstrated an increased ability  
225 of heat killed *E. faecalis* to accelerate diet-induced hyperlipidaemia. This suggests that there is  
226 variability in hyperlipidaemia accelerating potential amongst Gram positive organisms in zebrafish  
227 embryos. The basis of this difference could be further explored using model Gram positive  
228 organisms and Gram-positive organisms that are natural commensals in the zebrafish gut.

229

230 *Caenorhabditis elegans* fed with *S. maltophilia* accumulate neutral lipids within intracellular lipid  
231 droplets driven by a bacterially-encoded mechanism that is independent of the innate immune  
232 response<sup>19</sup>. Our finding that two distinct mouse-associated *S. maltophilia* strains were able to  
233 increase the hyperlipidaemic potential of chicken egg yolk suggests the digestive ability of *S.*  
234 *maltophilia* is potentially conserved between strains and potentially between host species.  
235 Previous studies have identified *S. maltophilia* strains within zebrafish gut microbiomes<sup>9</sup>, these  
236 zebrafish-associated strains could be analysed to determine if increased lipid uptake is a  
237 consequence of natural host-*S. maltophilia* pairs.

238

239 We also found an embryo growth-enhancing effect of pre-digesting commercially available  
240 zebrafish embryo feed with *S. maltophilia* which suggests *S. maltophilia* could have commercial  
241 applications as an aquaculture feed additive. The use of *S. maltophilia* as a feed additive is  
242 potentially risky as this organism is associated with opportunistic infections in humans and is  
243 resistant to a wide range of antibiotics<sup>20,21</sup>.

244

245 As a proof-of-principle study, our work demonstrates the feasibility of studying the interaction of  
246 transplanted pathobiont species, from a mammalian host, with an environmental factor to result  
247 in a conditional pathological phenotype in the tractable zebrafish model system. Further work is

248 required to examine effects of the two pathobiont species identified in our study on mammalian  
249 models of cardiovascular disease and to correlate their colonisation with the progression of  
250 cardiovascular disease phenotypes in mammalian models and human samples.

251

## 252 **Methods**

### 253 Zebrafish handling

254 Adult zebrafish were housed at the Centenary Institute (Sydney Local Health District Animal  
255 Welfare Committee Approval 17-036). Zebrafish embryos were obtained by natural spawning and  
256 conventionally raised embryos were maintained in E3 media at 28°C.

257

### 258 Generation of microbiome-depleted (MD) zebrafish embryos

259 Microbiome-depleted (MD) zebrafish were created and maintained as previously described <sup>22</sup>.  
260 Briefly, freshly laid embryos were rinsed with 0.003% v/v bleach in sterile E3 and rinsed 3 times  
261 with sterile E3. Bleached embryos were raised in sterile E3 supplemented with 50 µg/mL ampicillin  
262 (Sigma), 5 µg/mL kanamycin (Sigma) and 250 ng/mL amphotericin B (Sigma) in sterile tissue  
263 culture flasks. Dead embryos and chorions were aseptically removed at one and three dpf  
264 respectively.

265

266 Conventionalised zebrafish were used as a control, where 3 dpf MD zebrafish were inoculated  
267 with system water from the aquarium at Centenary Institute.

268

### 269 Generation of mouse faecal microbiota specimens

270 Mice were housed at the Centenary Institute (Sydney Local Health District Animal Welfare  
271 Committee Approval 2018/016). C57BL/6J mice were housed in a pathogen-free and temperature-  
272 controlled environment, with 12 hours of light and 12 hours of darkness, and free access to food

273 and water. Mice were provided with a High Fat Diet (HFD) or chow from 6 to 30 weeks of age. The  
274 HFD was prepared in-house based on rodent diet no. D12451 (Research Diets New Brunswick,  
275 USA) and its calories were supplied as: fat 45%, protein 20%, and carbohydrate 35%<sup>23</sup>. The chow  
276 diet was commercially produced by Speciality Feeds as “Irradiated Rat and Mouse Diet” and its  
277 calories were supplied as: fat 12%, protein 23%, and carbohydrate 65%.

278

279 Faecal pellets were collected from mice that were housed in different cages. Individual faecal  
280 pellets were collected into sterile 1.7 mL microcentrifuge tubes and homogenised in 1 mL of sterile  
281 E3 by pipetting. Homogenised specimens were centrifuged at 500 G for 2 minutes to sediment  
282 fibrous material and the supernatant was collected. Supernatants were supplemented with  
283 glycerol to a final concentration of 25% v/v, aliquoted, and frozen at -80°C for experimental use.

284

#### 285 Colonisation of zebrafish with mouse faecal microbiota

286 MD zebrafish were colonised at 3 dpf by transfer into sterile E3 and addition of 200 µL thawed  
287 faecal homogenate supernatant. At 5 dpf, embryos were rinsed with E3 and placed on a chicken  
288 egg yolk diet.

289

#### 290 Neutral red staining and morphology measurements

291 Neutral red staining was performed as previously described<sup>24</sup>. Briefly, 2.5 µg/mL neutral red was  
292 added to the media of 4 dpf embryos and incubated overnight. Embryos were rinsed with fresh E3  
293 to remove unbound neutral red and live imaged on a Leica M205FA microscope with a consistent  
294 zoom between specimens in a single experiment. The area of neutral red-stained midgut was  
295 measured in pixels using ImageJ. Body size was measured in pixels using ImageJ.

296

#### 297 Zebrafish high fat diet challenge with chicken egg yolk

298 High fat diet challenge with chicken egg yolk was performed as previously described<sup>25</sup>. Briefly, 5  
299 dpf zebrafish embryos were placed in an E3 solution containing 0.05% w/v emulsified hard boiled  
300 chicken egg yolk in glass beakers. Beakers were housed in a 28°C incubator with a 14:10 hour  
301 light:dark cycle. The emulsified hard boiled chicken egg yolk solution was changed daily.

302

### 303 Oil Red O staining assay

304 Oil Red O staining and analysis was performed as previously described<sup>25-27</sup>. Briefly, 7 dpf embryos  
305 were fixed overnight at 4°C in 4% paraformaldehyde, rinsed with PBS, and rinsed stepwise through  
306 to propylene glycol. Embryos were stained with filtered 0.5% (w/v) Oil Red O dissolved in  
307 propylene glycol overnight at room temperature. Unbound dye was removed by washing with  
308 propylene glycol and embryos were rinsed stepwise through to PBS for imaging.

309

310 Embryos were imaged on a Leica M205FA microscope. Experimental batches of colour images  
311 were analysed in ImageJ by adjusting the colour threshold function to eliminate non-red signal,  
312 this output was then converted to a binary mask and the tail region posterior to the swim bladder  
313 was selected to measure the area of particles.

314

### 315 Isolation, identification, and handling of bacterial isolates from mouse faecal microbiota samples

316 Faecal homogenate supernatants were plated onto LB Agar (Amyl Media) and incubated at 28°C  
317 for two days. Individual isolates were grown in broth culture in Luria Broth (Miller's LB Broth Base,  
318 Thermofisher) at 28°C overnight with 200 RPM shaking.

319

320 For identification, bacteria were harvested from broth culture and subjected to PCR using  
321 universal 16S primers (5'-3') Fw Rv. PCR products were sequenced by Sanger Sequencing (AGRF)

322 and NCBI records were searched by BLAST to identify the closest matching bacterial strain by  
323 sequence identity.

324

325 For gnotobiotic experiments, bacteria were harvested from overnight broth cultures and  
326 resuspended in sterile E3 zebrafish embryo media at a concentration of OD600 0.2. MD zebrafish  
327 in autoclaved E3 were then inoculated with the bacterial suspension at a ratio of 1:200.

328

329 For heat killed bacterial inoculations, bacteria were resuspended in E3 at a concentration of  
330 OD600 0.2 and heat-killed in a 95°C heat block for 30 minutes. Heat killed bacterial solutions were  
331 then added at 1:200 ratio to 3 dpf MD zebrafish.

332

333 For purified ligand exposure, 3 dpf MD zebrafish were soaked in 25 µg/mL lipoteichoic acid  
334 (Sigma) or 25 µg/mL peptidoglycan (Sigma).

335

336 For lysozyme digestion of heat-killed *E. faecalis*, a suspension of heat-killed bacteria was incubated  
337 with 50 µg/mL lysozyme (Sigma) at 37°C for 6 h before being used to inoculate 3 dpf MD zebrafish  
338 at a ratio of 1:200.

339

#### 340 Gene knockdown with CRISPR-Cas9

341	gRNA	templates	for	<i>myd88</i>	(5`-	3`):	Target	1
342	TAATACGACTCACTATAGGCAGTTTCCGAAAGAACTGTTTTAGAGCTAGAAATAGC,						Target	2
343	TAATACGACTCACTATAGGAAAAGGTCTTGACGGACTGTTTTAGAGCTAGAAATAGC,						Target	3
344	TAATACGACTCACTATAGGAACTGTTTGATCATCTCGGTTTTAGAGCTAGAAATAGC,						Target	4
345	TAATACGACTCACTATAGGTTTTTTTCGATAAGCTCACGTTTTAGAGCTAGAAATAGC.						gRNA	was

346 synthesized as previously described <sup>28</sup>.

347

348 A 1:1 solution of gRNA and 500 µg/mL of Cas9 nuclease V3 (Integrated DNA Technology) was  
349 prepared with phenol red dye (Sigma, P0290). Freshly laid eggs were collected from breeding  
350 tanks and the solution was injected in the yolk sac of the egg before the emergence of the first cell  
351 with a FemtoJet 4i (Eppendorf).

352

353 Knockdown efficacy was monitored by RT-qPCR as previously described<sup>29</sup>. *myd88*-specific primers  
354 (5`-3`): Fw ACAGGGACTGACACCTGAGA, Rv GACGACAGGGATTAGCCGTT.

355

356 To derive MD crispant embryos, injected embryos were placed in E3 containing ampicillin,  
357 kanamycin and amphotericin B as described previously. Bleaching injected embryos caused high  
358 mortality rates.

359

#### 360 Digestion of chicken egg yolk

361 20 g hard-boiled chicken egg yolk was mixed with 40 mL E3 and emulsified using a Branson Digital  
362 Sonifier sonicator. Emulsified egg yolk was inoculated with bacterial isolates in E3 (described  
363 above) at a 1:200 ratio. Egg yolk mixture was then placed in a shaker at 28 °C at 200 rpm and for  
364 48 h. Samples were then autoclaved prior to feeding experiments.

365

#### 366 Analysis of chicken egg yolk composition

367 “Pre-digested” samples were autoclaved and mailed to Australian Laboratory Services (VIC,  
368 Australia) for commercial grade nutritional analyses.

369

#### 370 Statistics

371 All statistical analyses (t-tests and ANOVA where appropriate) were performed using GraphPad  
372 Prism 8. Outliers were removed using ROUT, with Q = 1%. All data shown are representative of at  
373 least 2 biological replicates.

374

#### 375 **Data availability**

376 Source data are provided with this paper.

377 Raw image and analysis data is archived for 10 years by The Centenary Institute and available on  
378 request from the corresponding author (Sydney, Australia).

379

#### 380 **Acknowledgements**

381 Funding: Australian National Health and Medical Research Council Project Grant APP1099912; The  
382 University of Sydney Fellowship G197581; NSW Ministry of Health under the NSW Health Early-  
383 Mid Career Fellowships Scheme H18/31086 to SHO. Australian National Health and Medical  
384 Research Council Centres of Research Excellence Grant APP1153493 to WJB. The funders had no  
385 role in study design, data collection and analysis, decision to publish, or preparation of the  
386 manuscript.

387

388 The *E. faecalis* UNSW 054400 type strain was provided by Dr Laurence Marcia.

389

390 The authors acknowledge the facilities and the technical assistance of Dr Angela Kurz at the  
391 Biolmaging Facility and Sydney Cytometry at Centenary Institute.

392

393 The authors declare no conflicts of interest.

394

#### 395 **References**



- 396 1 Sekirov, I., Russell, S. L., Antunes, L. C. & Finlay, B. B. Gut microbiota in health and disease.  
397 *Physiol Rev* **90**, 859-904, doi:10.1152/physrev.00045.2009 (2010).
- 398 2 Backhed, F., Manchester, J. K., Semenkovich, C. F. & Gordon, J. I. Mechanisms underlying  
399 the resistance to diet-induced obesity in germ-free mice. *Proc Natl Acad Sci U S A* **104**, 979-  
400 984, doi:10.1073/pnas.0605374104 (2007).
- 401 3 Arias-Jayo, N. *et al.* High-Fat Diet Consumption Induces Microbiota Dysbiosis and Intestinal  
402 Inflammation in Zebrafish. *Microb Ecol* **76**, 1089-1101, doi:10.1007/s00248-018-1198-9  
403 (2018).
- 404 4 Rawls, J. F., Mahowald, M. A., Ley, R. E. & Gordon, J. I. Reciprocal gut microbiota  
405 transplants from zebrafish and mice to germ-free recipients reveal host habitat selection.  
406 *Cell* **127**, 423-433 (2006).
- 407 5 Murphy, E. A., Velazquez, K. T. & Herbert, K. M. Influence of high-fat diet on gut  
408 microbiota: a driving force for chronic disease risk. *Curr Opin Clin Nutr Metab Care* **18**, 515-  
409 520, doi:10.1097/MCO.000000000000209 (2015).
- 410 6 Ridaura, V. K. *et al.* Gut microbiota from twins discordant for obesity modulate metabolism  
411 in mice. *Science* **341**, 1241214, doi:10.1126/science.1241214 (2013).
- 412 7 Lopez Nadal, A. *et al.* Feed, Microbiota, and Gut Immunity: Using the Zebrafish Model to  
413 Understand Fish Health. *Frontiers in immunology* **11**, 114, doi:10.3389/fimmu.2020.00114  
414 (2020).
- 415 8 Brinkmann, B. W., Koch, B. E. V., Spaik, H. P., Peijnenburg, W. & Vijver, M. G. Colonizing  
416 microbiota protect zebrafish larvae against silver nanoparticle toxicity. *Nanotoxicology* **14**,  
417 725-739, doi:10.1080/17435390.2020.1755469 (2020).
- 418 9 Stressmann, F. A. *et al.* Mining zebrafish microbiota reveals key community-level resistance  
419 against fish pathogen infection. *ISME J* **15**, 702-719, doi:10.1038/s41396-020-00807-8  
420 (2021).
- 421 10 Valenzuela, M. J. *et al.* Evaluating the Capacity of Human Gut Microorganisms to Colonize  
422 the Zebrafish Larvae (*Danio rerio*). *Front Microbiol* **9**, 1032, doi:10.3389/fmicb.2018.01032  
423 (2018).
- 424 11 Bates, J. M. *et al.* Distinct signals from the microbiota promote different aspects of  
425 zebrafish gut differentiation. *Dev Biol* **297**, 374-386, doi:S0012-1606(06)00774-3 [pii]  
426 10.1016/j.ydbio.2006.05.006 (2006).
- 427 12 Oehlers, S. H. *et al.* A chemical enterocolitis model in zebrafish larvae that is dependent on  
428 microbiota and responsive to pharmacological agents. *Dev Dyn* **240**, 288-298,  
429 doi:10.1002/dvdy.22519 (2011).
- 430 13 Cheesman, S. E., Neal, J. T., Mittge, E., Seredick, B. M. & Guillemin, K. Epithelial cell  
431 proliferation in the developing zebrafish intestine is regulated by the Wnt pathway and  
432 microbial signaling via Myd88. *Proc Natl Acad Sci U S A* **108 Suppl 1**, 4570-4577,  
433 doi:1000072107 [pii]  
434 10.1073/pnas.1000072107 (2011).
- 435 14 Novoa, B., Bowman, T. V., Zon, L. & Figueras, A. LPS response and tolerance in the zebrafish  
436 (*Danio rerio*). *Fish Shellfish Immunol* **26**, 326-331, doi:S1050-4648(08)00293-3 [pii]  
437 10.1016/j.fsi.2008.12.004 (2009).
- 438 15 Kaye, D. M. *et al.* Deficiency of Prebiotic Fiber and Insufficient Signaling Through Gut  
439 Metabolite-Sensing Receptors Leads to Cardiovascular Disease. *Circulation* **141**, 1393-1403,  
440 doi:10.1161/CIRCULATIONAHA.119.043081 (2020).
- 441 16 Tan, F. *et al.* The Responses of Germ-Free Zebrafish (*Danio rerio*) to Varying Bacterial  
442 Concentrations, Colonization Time Points, and Exposure Duration. *Front Microbiol* **10**,  
443 2156, doi:10.3389/fmicb.2019.02156 (2019).

- 444 17 Weitekamp, C. A. *et al.* Monoassociation with bacterial isolates reveals the role of  
445 colonization, community complexity and abundance on locomotor behavior in larval  
446 zebrafish. *Anim Microbiome* **3**, 12, doi:10.1186/s42523-020-00069-x (2021).
- 447 18 Robinson, C. D. *et al.* Experimental bacterial adaptation to the zebrafish gut reveals a  
448 primary role for immigration. *PLoS Biol* **16**, e2006893, doi:10.1371/journal.pbio.2006893  
449 (2018).
- 450 19 Xie, K. *et al.* Dietary *S. maltophilia* promotes fat storage by enhancing  
451 lipogenesis and ER-LD contacts in *C. elegans*. *bioRxiv*, 2020.2004.2029.067793,  
452 doi:10.1101/2020.04.29.067793 (2020).
- 453 20 Brooke, J. S. *Stenotrophomonas maltophilia*: an emerging global opportunistic pathogen.  
454 *Clin Microbiol Rev* **25**, 2-41, doi:10.1128/CMR.00019-11 (2012).
- 455 21 Pathmanathan, A. & Waterer, G. W. Significance of positive *Stenotrophomonas maltophilia*  
456 culture in acute respiratory tract infection. *Eur Respir J* **25**, 911-914,  
457 doi:10.1183/09031936.05.00096704 (2005).
- 458 22 Melancon, E. *et al.* Best practices for germ-free derivation and gnotobiotic zebrafish  
459 husbandry. *Methods Cell Biol* **138**, 61-100, doi:10.1016/bs.mcb.2016.11.005 (2017).
- 460 23 Henderson, J. M. *et al.* Multiple liver insults synergize to accelerate experimental  
461 hepatocellular carcinoma. *Scientific reports* **8**, 10283, doi:10.1038/s41598-018-28486-8  
462 (2018).
- 463 24 Oehlers, S. H. *et al.* Chemically induced intestinal damage models in zebrafish larvae.  
464 *Zebrafish* **10**, 184-193, doi:10.1089/zeb.2012.0824 (2013).
- 465 25 Morris, S., Cholan, P., Britton, W. J. & Oehlers, S. H. Glucose inhibits neutrophil migration  
466 and haemostasis, and accelerates diet-induced hyperlipidaemia in zebrafish embryos.  
467 *bioRxiv*, 2021.2001.2028.428551, doi:10.1101/2021.01.28.428551 (2021).
- 468 26 Fang, L. *et al.* In vivo visualization and attenuation of oxidized lipid accumulation in  
469 hypercholesterolemic zebrafish. *J Clin Invest*, doi:10.1172/JCI57755 (2011).
- 470 27 Johansen, M. D. *et al.* Mycobacterium marinum infection drives foam cell differentiation in  
471 zebrafish infection models. *Dev Comp Immunol* **88**, 169-172, doi:10.1016/j.dci.2018.07.022  
472 (2018).
- 473 28 Wu, R. S. *et al.* A Rapid Method for Directed Gene Knockout for Screening in G0 Zebrafish.  
474 *Dev Cell* **46**, 112-125 e114, doi:10.1016/j.devcel.2018.06.003 (2018).
- 475 29 Cholan, P. M. *et al.* Conserved anti-inflammatory effects and sensing of butyrate in  
476 zebrafish. *Gut Microbes* **12**, 1-11, doi:10.1080/19490976.2020.1824563 (2020).
- 477

## 478 **Figure Legends**

479 Figure 1: Transplantation of microbiota from HFD-fed mice accelerates hyperlipidaemia in  
480 zebrafish embryos.

481 (a) Schematic describing method of faecal microbiome inoculation in MD zebrafish and chicken  
482 egg yolk challenge diet. (b) Representative images of neutral red staining in mid-gut of 5 dpf  
483 zebrafish embryos. Red brackets indicate mid-gut region used for quantification. (c) Quantification  
484 of neutral red staining area in mid-gut of 5 dpf zebrafish embryos. (d) Representative images of Oil

485 Red O staining of 7 dpf chow-fed and HFD-fed mouse faecal microbiome-inoculated zebrafish  
486 embryos. Red brackets indicate tail region posterior to the swim bladder used for quantification  
487 (e) Quantification of trunk vascular Oil Red O staining from the tail region posterior to the swim  
488 bladder in MD zebrafish inoculated with mouse faecal microbiota and challenged with chicken egg  
489 yolk diet from 5-7 dpf. Scale bar represents 500  $\mu$ m. Results are expressed as mean  $\pm$  SD.

490

491 Figure 2: Identification of individual microbes with pathobiont activity.

492 (a) Schematic describing workflow to isolate *Escherichia species* PYCC8248 (*E.s*), *Escherichia coli*  
493 strain Y15 (*E.c*), *Stenotrophomonas maltophilia* strain CD103 (*S.m*) and *Enterococcus faecalis* strain  
494 YN771 (*E.f*) and inoculate into MD zebrafish with subsequent chicken egg yolk diet challenge. (b)  
495 Quantification of trunk vascular Oil Red O staining from the tail region posterior to the swim  
496 bladder in MD zebrafish inoculated with bacterial isolates *E.s*, *E.c*, *S.m*, and *E.f* and challenged with  
497 a chicken egg yolk diet from 5-6 dpf. (c) Area of neutral red stained in the mid-gut of 5 dpf  
498 gnotobiotic zebrafish embryos mono-associated with bacterial isolates *E.s*, *E.c*, *S.m* and *E.f*. (d)  
499 Quantification of trunk vascular Oil Red O staining from the tail region posterior to the swim  
500 bladder in MD zebrafish inoculated with bacterial isolates *E.f*, *E. faecalis* UNSW 054400 type strain  
501 (*E.f* UNSW), *S.m* and *S. maltophilia* yy01 (*S.m* yy01) and challenged with a chicken egg yolk diet  
502 from 5-6 dpf. Results are expressed as mean  $\pm$  SD.

503

504 Figure 3: *Enterococcus faecalis* (*E.f*) accelerates hyperlipidaemia by activating host immune  
505 signalling pathways.

506 (a) Schematic describing inoculation of MD zebrafish embryos with heat-killed bacterial isolates  
507 *E.s*, *E.c*, *S.m* and *E.f* from 3-5 dpf, followed by chicken egg yolk diet challenge from 5-7 dpf. (b)  
508 Quantification of trunk vascular Oil Red O staining from the tail region posterior to the swim  
509 bladder in MD zebrafish inoculated with heat killed bacterial isolates *E.s*, *E.c*, *S.m*, and *E.f* and

510 challenged with a chicken egg yolk diet. (c) Quantification of *myd88* expression in zebrafish  
511 embryos injected with *myd88*-targeting CRISPR-Cas9 complexes at 5 dpf. Each dot represents a  
512 biological replicate of at least 10 embryos. (d) Quantification of trunk vascular Oil Red O staining  
513 from the tail region posterior to the swim bladder in control scrambled and *myd88* crisprant  
514 embryos exposed to *E.f* and challenged with a chicken egg yolk diet. Results are expressed as  
515 mean  $\pm$  SD.

516

517 Figure 4: Gram-positive cell wall components accelerate hyperlipidaemia in zebrafish embryos.

518 (a) Quantification of trunk vascular Oil Red O staining from the tail region posterior to the swim  
519 bladder in MD zebrafish inoculated with heat killed bacterial isolates *E.f* and *Staphylococcus*  
520 *xylosus* (*S.x*) from 3-5 dpf and challenged with a chicken egg yolk diet from 5-7 dpf. (b)  
521 Quantification of trunk vascular Oil Red O staining from the tail region posterior to the swim  
522 bladder in MD zebrafish pre-incubated with LTA or peptidoglycan from 3-5 dpf before co-  
523 challenge with chicken egg yolk diet from 5-7 dpf. (c) Quantification of trunk vascular Oil Red O  
524 staining from the tail region posterior to the swim bladder in MD zebrafish pre-incubated with  
525 lysozyme-treated heat killed *E.f* from 3-5 dpf and challenged with a chicken egg yolk diet from 5-7  
526 dpf. (d) Quantification of trunk vascular Oil Red O staining from the tail region posterior to the  
527 swim bladder in control scrambled and *myd88* crisprant embryos pre-incubated with LTA or  
528 peptidoglycan from 3-5 dpf before co-challenge with chicken egg yolk diet from 5-7 dpf. Results  
529 are expressed as mean  $\pm$  SD.

530

531 Figure 5: *Stenotrophomonas maltophilia* accelerates hyperlipidaemia by digesting food.

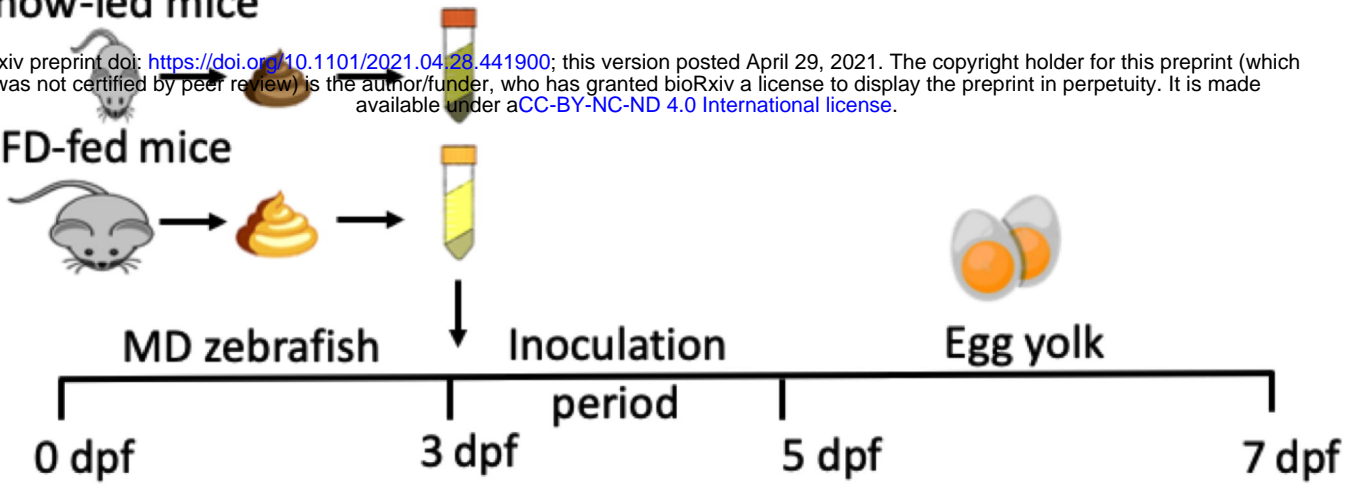
532 (a) Schematic describing creation of “pre-digested” chicken egg yolk by incubation with bacterial  
533 isolates *E.s*, *E.c*, *S.m*, and *E.f*, autoclaving, for feeding to 5-7 dpf zebrafish embryos. (b)  
534 Quantification of trunk vascular Oil Red O staining from the tail region posterior to the swim

535 bladder in MD zebrafish fed “pre-digested” egg yolk with bacterial isolates *E.s*, *E.c*, *S.m*, and *E.f*  
536 from 5-7 dpf. (c) Quantification of trunk vascular Oil Red O staining from the tail region posterior  
537 to the swim bladder in conventionally raised zebrafish fed “pre-digested” egg yolk with bacterial  
538 isolate *S.m* from 5-7 dpf. (d) Quantification of trunk vascular Oil Red O staining from the tail region  
539 posterior to the swim bladder in conventionally raised zebrafish fed “pre-digested” fish embryo  
540 food with bacterial isolates *E.c* and *S.m* from 5-7 dpf. (e) Representative images of “pre-digested”  
541 egg yolk with bacterial isolates *E.c* and *S.m* red brackets indicate fraction of the water column  
542 containing large particulates after autoclaving. (f) CFU recovery from chicken egg yolk “pre-  
543 digestion” reactions. Results are expressed as mean  $\pm$  SD.

# A Chow-fed mice

bioRxiv preprint doi: <https://doi.org/10.1101/2021.04.28.441900>; this version posted April 29, 2021. The copyright holder for this preprint (which was not certified by peer review) is the author/funder, who has granted bioRxiv a license to display the preprint in perpetuity. It is made available under aCC-BY-NC-ND 4.0 International license.

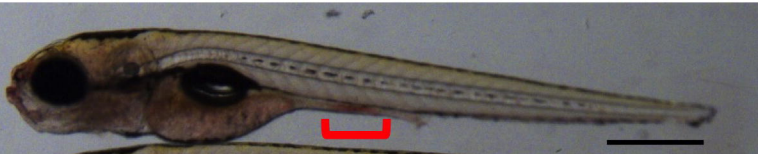
# HFD-fed mice



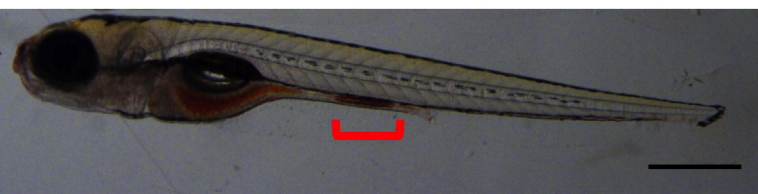
## B

### Neutral red staining

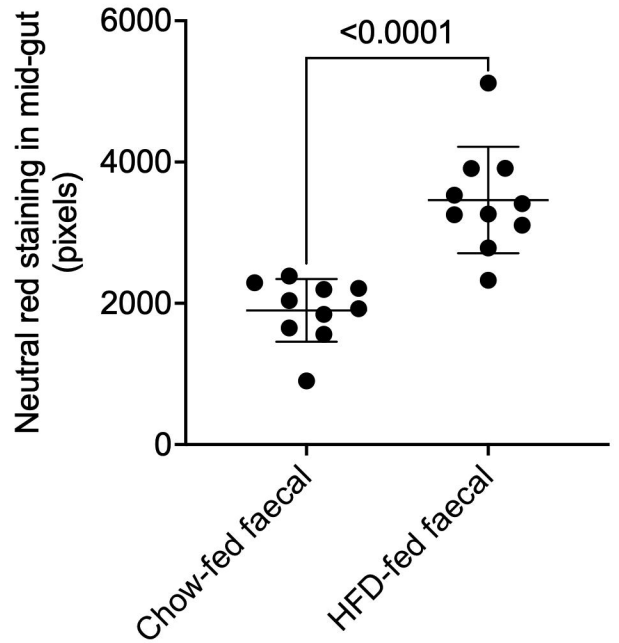
Chow-fed mouse faecal microbiome inoculated zebrafish



HFD-fed mouse faecal microbiome inoculated zebrafish



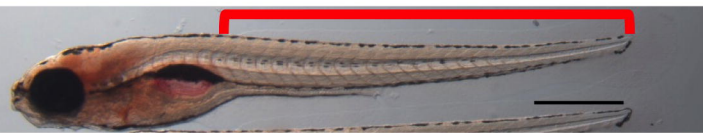
## C



## D

### Oil Red O staining

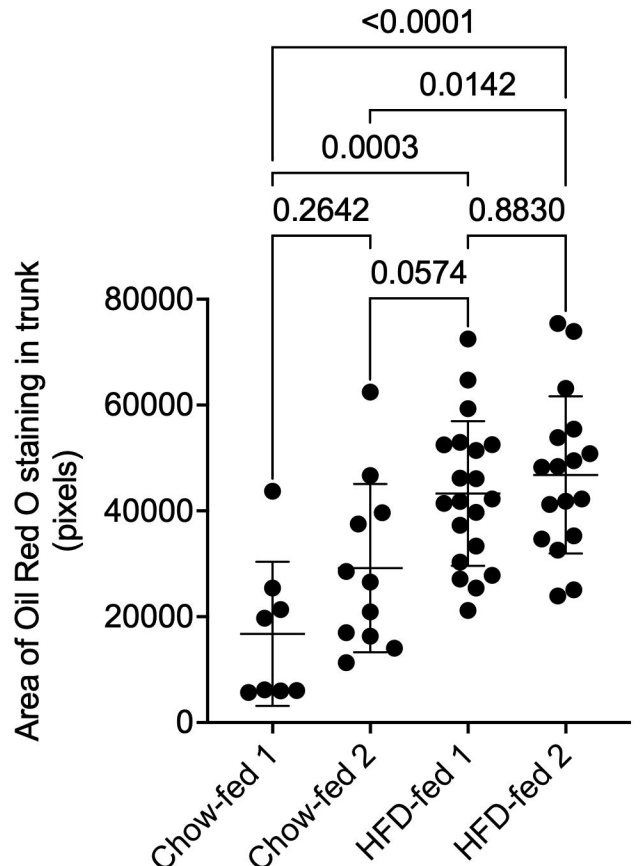
Chow-fed mouse faecal microbiome inoculated zebrafish

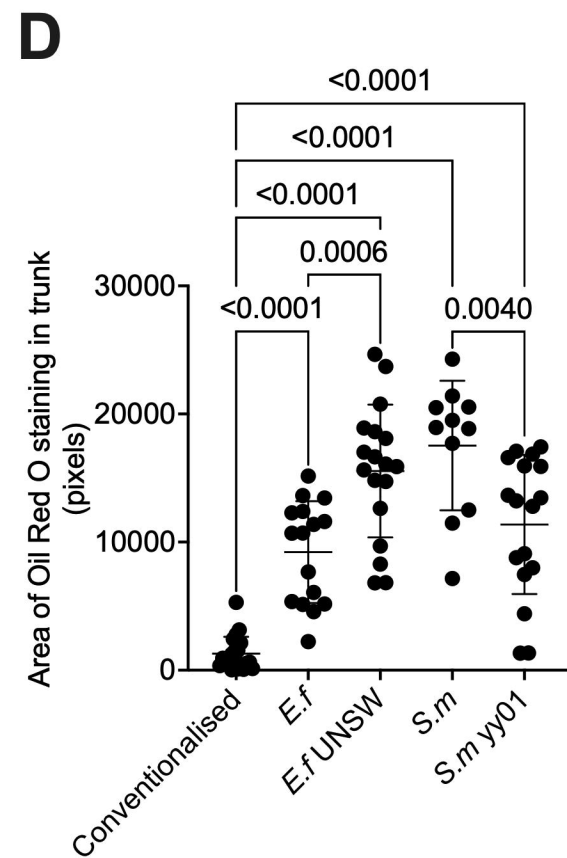
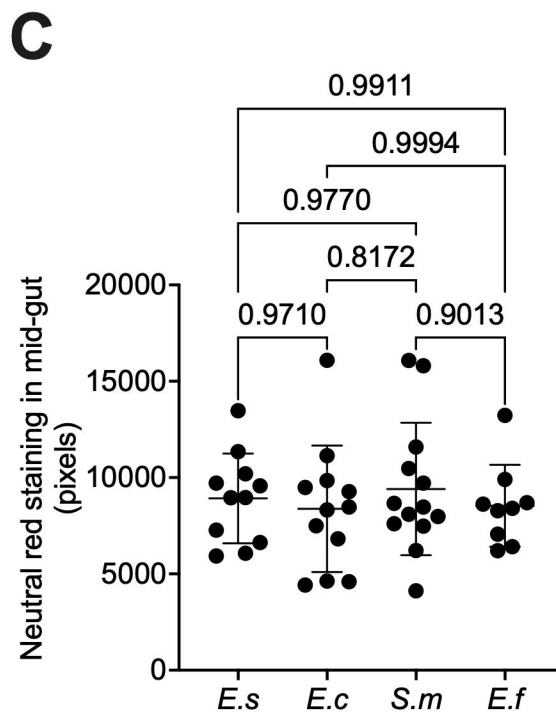
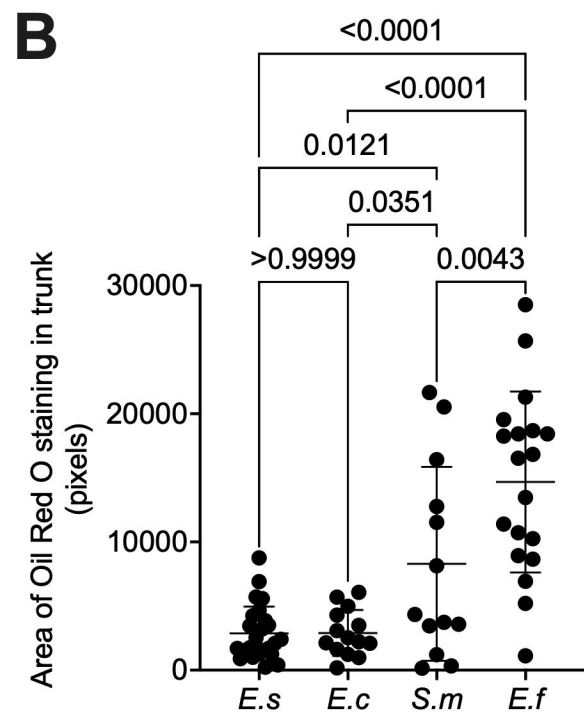
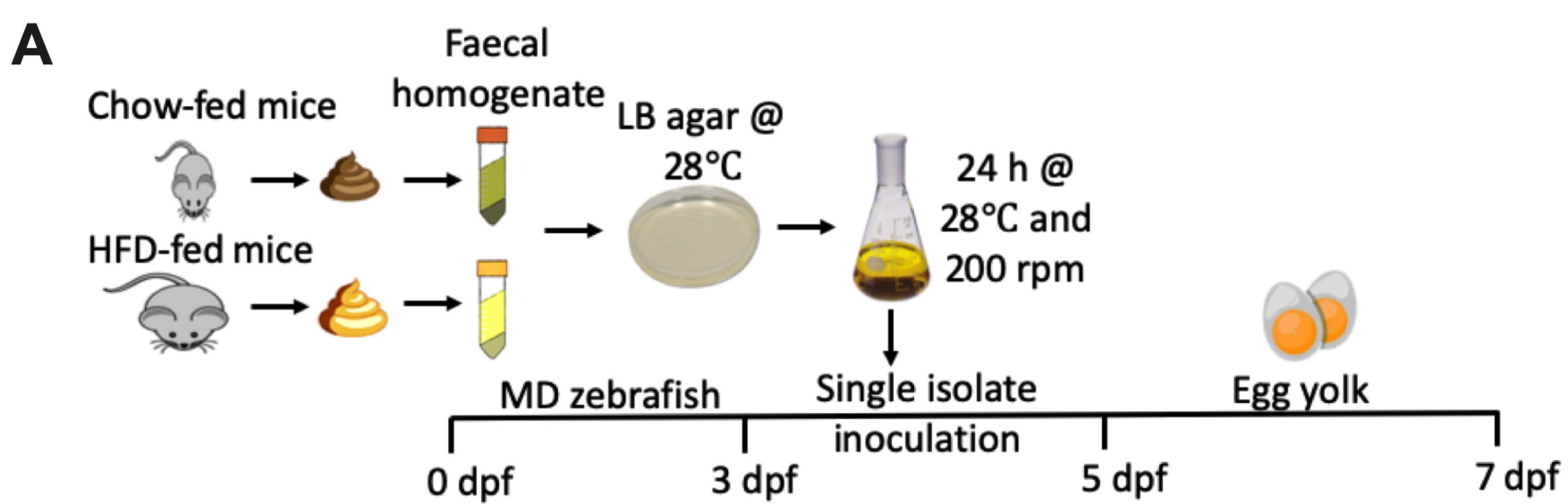


HFD-fed mouse faecal microbiome inoculated zebrafish

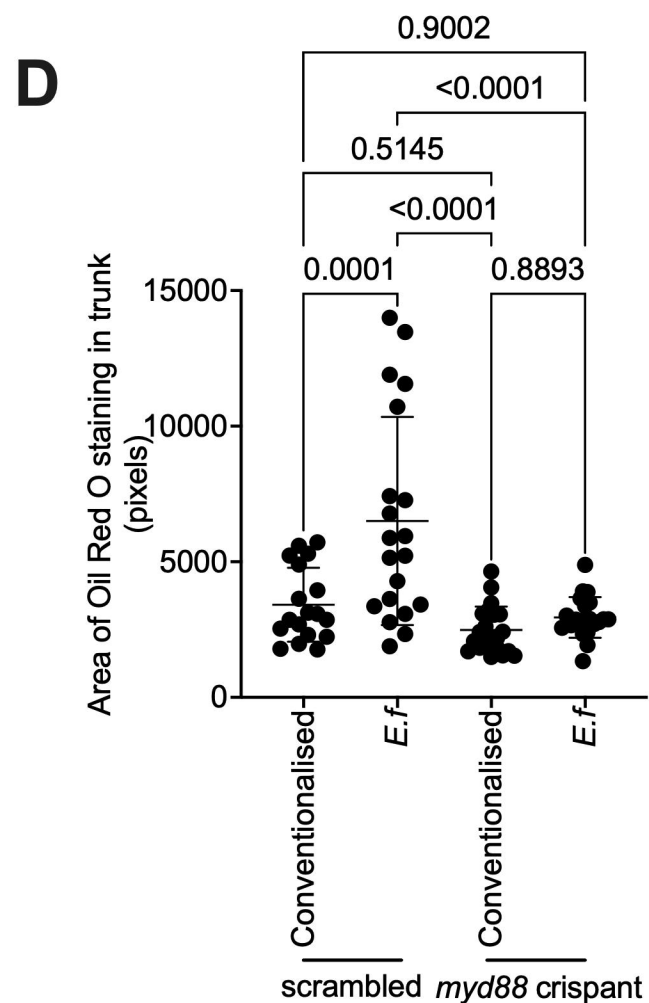
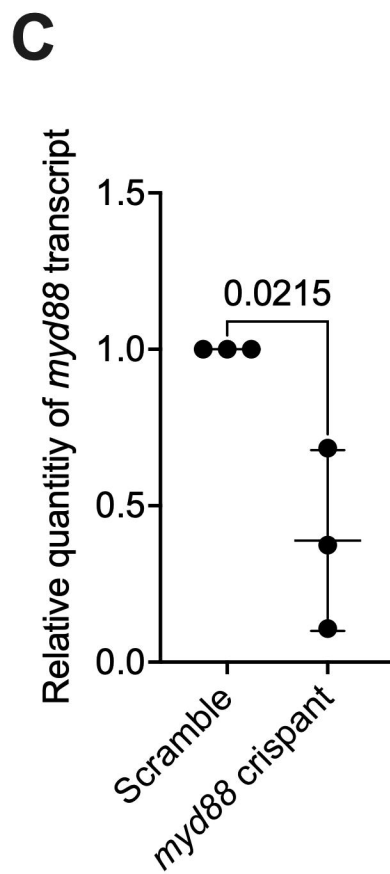
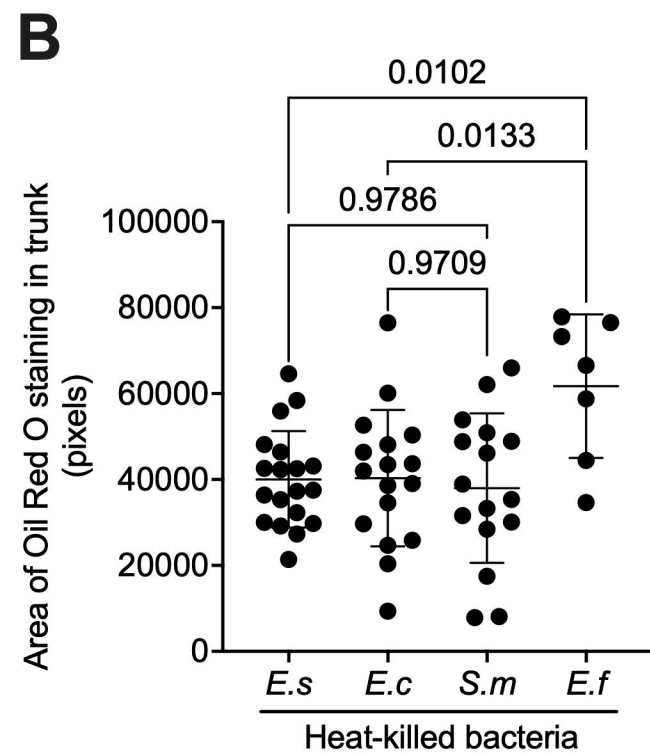
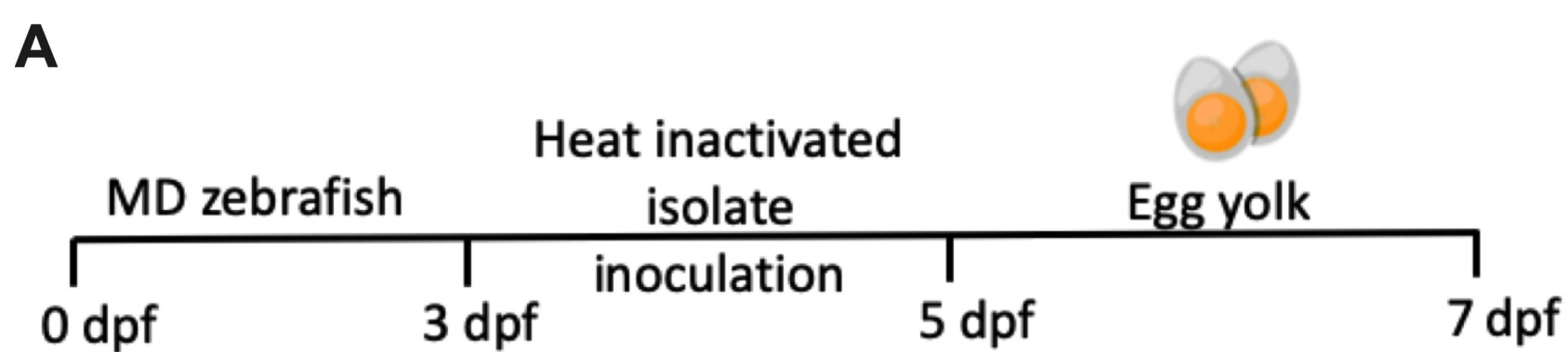


## E

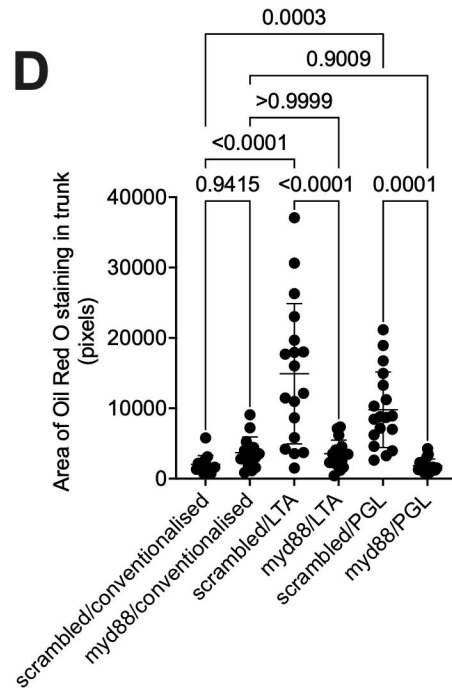
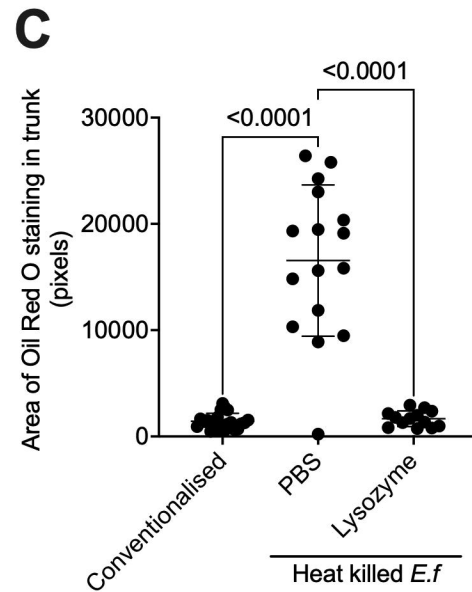
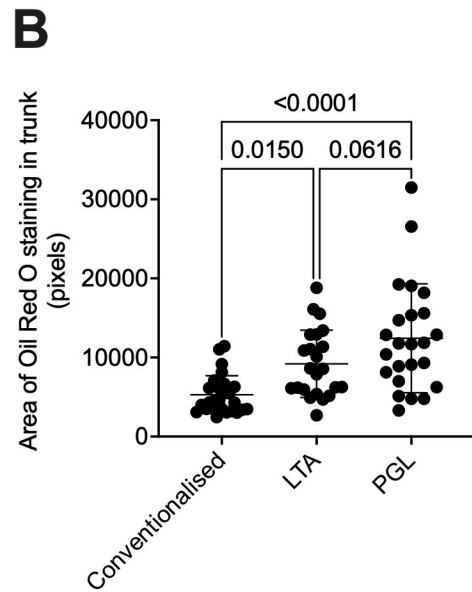
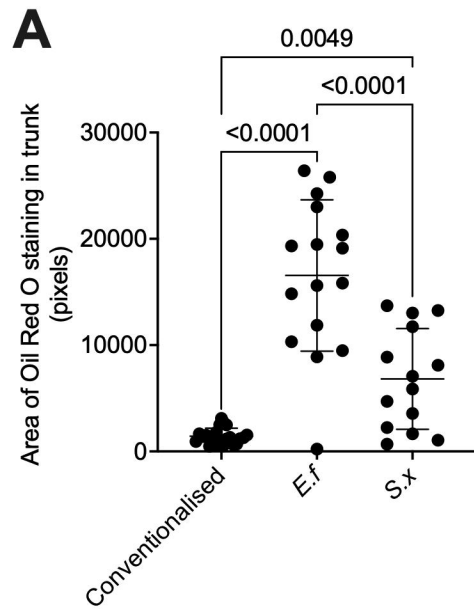


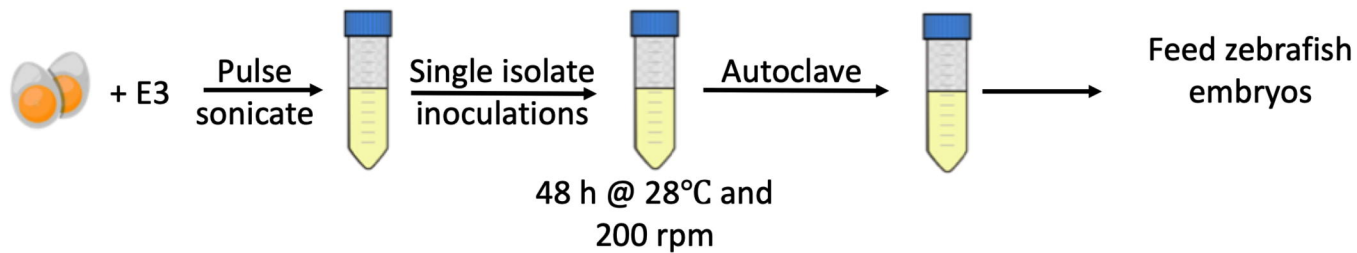
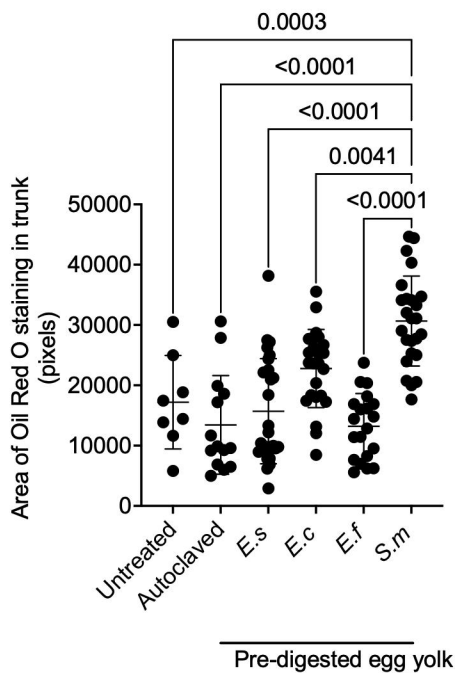
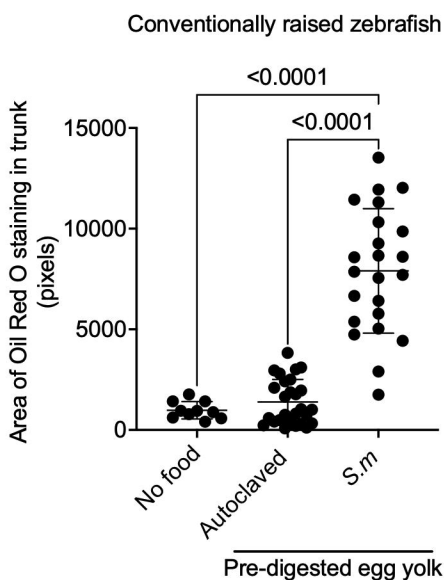
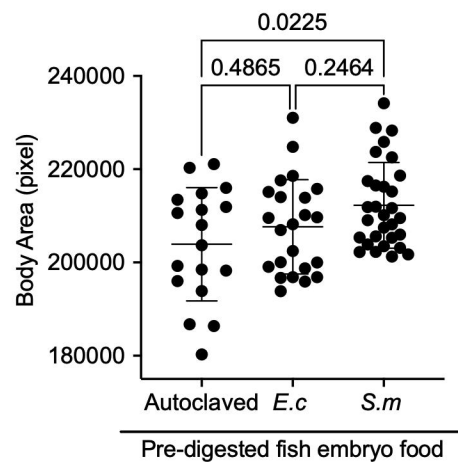
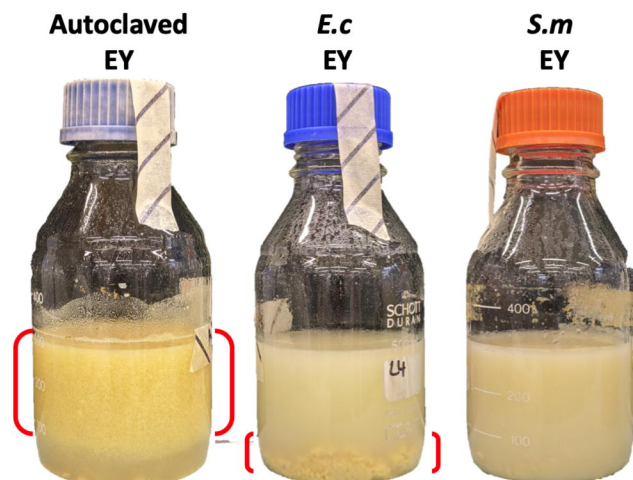










**A****B****C****D****E****F**